

The influence of substrate location and deposition time on ZnO nanostructures

Khalifa Al-Azri*, Roslan Md Nor, Majid.S.Al-Ruqeishi and Y. M. Amin

Department of physics, Faculty of Science, University Malaya 50603 Kuala Lumpur, Malaysia

*ay3579@yahoo.com Tel: +603-79674206 Fax: +603-79674146 (Corresponding author). Received on 18th June 2009, accepted in revised form 20th July 2010.

ABSTRACT A study on the formation of ZnO nanostructures using the carbothermal evaporation method without catalyst and at atmospheric argon pressure has been conducted. The effects of the position of the substrates to the source and deposition time were investigated. The results of these parametric studies based on field-emission scanning electron microscopy (FESEM), Energy dispersive X-ray spectroscopy (EDX) spectrum and X-ray diffraction (XRD) analyses support the reduction-evaporation model for ZnO nanostructures formation using carbothermal evaporation.

(**Keywords:** ZnO; nanostructures; carbothermal evaporation)

INTRODUCTION

Zinc oxide (ZnO) has attracted extensive research efforts because it exhibits many unique interesting properties, including anisotropy in crystal structure, nonstoichiometric defect structures, a direct wide band gap (3.37eV) at room temperature and large exciton binding energy of 60 meV [1].

Based on the unique properties of ZnO nanostructures, there are many novel applications have been appeared. For example, ZnO wires have been applied to construct Schottky diodes [2], field effect transistors (FET) [3] and light emitting diodes (LEDs) [4]. In recent years, number of different morphologies and fabrication methods for ZnO nanostructures were demonstrated.

Up to now, various ZnO nanostructures including nanowires [5], nanorods [6], nanotubes [7], nanoribbons [8], nanobelts [9] have been reported. Typically, good quality ZnO materials have been reported by different methods, including organic chemical vapor-phase epitaxy [10], carbothermal reactions [11], infrared irradiation, thermal evaporation and thermal decomposition [12,13] and laser assisted vapor-liquid-solid growth [14].

Among these, carbothermal reactions method give many advantages such as simplicity, economical and suitable for high yield production of ZnO nanostructures. However, some problems have been reported [15] in synthesized ZnO nanostructures including metal contamination during the growth process that affect negatively the properties of ZnO nanostructures. Thus, researchers have developed some processes to

synthesize ZnO nanostructures without any catalysts [16,17].

In addition, ZnO nanostructures exhibit a wide range of electrical and optical properties that depend sensitively on both shape and size, and both of fundamental and technological interest. For that reason, understanding the relationship between the effects of different growth parameters and the growth mechanism is very important for controlling the size and the shape of ZnO nanostructures.

In this paper, we reported a chemical vapor transport and condensation (CVTC) route to synthesize ZnO nanostructures without catalyst and at atmospheric pressure. In addition, the effects of experiment parameters such as the substrate locations and deposition time on the mechanism growth have been investigated.

Experimental Setup

In the typical growth process, n-type Si (100) wafers were used as substrates for growth of ZnO nanostructures. Before the growth process, the silicon substrates were dipped in sonicating bath of acetone for 15 minutes and rinsed with deionized water.

The experimental system consisted of a horizontal tube furnace (110 cm long), a temperature controller, gas supply and control system. The horizontal tube was opened from one side to the air and other end linked to a gas supply and flow control system.

The source material was mixtures of high-purity ZnO (Sigma Aldrich 99.9%) and carbon powders (Sigma Aldrich 99.95%) with 1:1 molar ratio. A

porcelain boat (2 cm diameter, 8 cm long) with the ZnO/C mixture was placed into the horizontal tube and pushed to the center of the furnace.

Silicon substrate pieces were placed at different locations range from 6 to 19 cm downstream from the center. Deposition process was conducted at 1100 °C furnace temperature and the Ar (99.9%) flow rate was set at 40 standard cubic centimeters per minute (s.c.c.m.) for 15, 30, 45 and 60 minutes.

Due to the temperature gradient downstream, the temperature of substrate region was less than the source temperature. The quartz tube was drawn out from the furnace and cooled down to room temperature in the air. White and gray colors products were formed on the surface of the silicon wafers.

The as-grown ZnO nanostructures were characterized by field emission gun scanning electron microscopy (FESEM) (Quanta200F), Energy dispersive X-ray spectroscopy (EDX) spectrum (Oxford Inst), X-ray diffraction (XRD) (Siemens D-5000 diffractometer by using copper-monochromatized Cu K α 1 radiation ($\lambda=1.540598 \text{ \AA}$) under the accelerating voltage of 40 kV and the current of 40 mA.

RESULTS AND DISCUSSIONS

Effect of the location of the Si substrate

Typical FESEM images of the ZnO products obtained from the study of the substrates location variation are shown in figure 1. In figure 1(a), a complete film of ZnO was formed with particles of a few micrometers in size for the sample located at 6 cm away from the center. Figure 2 shows the corresponding (EDX) spectra for all the studied samples. Figure 2 (a) shows that the atomic % of Zn element was very small compared to silicon.

This indicates that at short distance from the source, the substrate has higher temperature than the boiling temperature of the Zn (907°C) and this leads to re-evaporated of Zn atoms from the substrate without being oxidized. At 11 cm away from the center aligned ZnO nanowires were formed on silicon substrate as illustrated in figure 1(b).

The average diameter of these nanowires was about 50 nm to 200 nm and the length was 4-8 μm . The EDX spectrum in figure 2(b) demonstrates that the percentage of Zn and oxygen were increased compared to silicon.

Figure 1(c) shows irregular shape of ZnO nanostructures with non-aligned nanowires were formed in large quantity for the sample at 15 cm far from the center.

The corresponding EDX result in figure 2(c) showed significant increase in the Zn and O peaks relative to the silicon peak. For the silicon substrate which was located 19 cm away from the center, microstructures in the form of disks were obtained as shown in figure 1(d). The corresponding EDX result as it is shown in figure 2(d), no oxygen peak was observed and the microstructures disks were only contented of Zn.

This is a direct evidence of the carbothermal mechanism of the ZnO nanostructures formation where reduction of ZnO occurred in ZnO/C mixture at elevated temperatures to produce Zn, which evaporated and redeposit on the substrates. In other words, ZnO nanostructures were formed upon silicon substrates via the oxidation of the deposit Zn.

Figure 3 shows the XRD patterns of the samples grown on Si (1 0 0) substrates at different locations from the center of the furnace. The strong intensity and narrow width of ZnO diffraction peaks indicate that the resulting products were of high crystallinity. On one hand, no diffraction peaks from metallic Zn or other impurities were detected in the samples located at 11 cm and 15 cm besides ZnO peaks.

Thus, the XRD diffraction peaks can be assigned to (100), (002), (101), (102), (103) and (112) standard hexagonal wurtzite structure of ZnO with cell parameter of $a = b = 3.249 \text{ \AA}$, and $c = 5.206 \text{ \AA}$ [18]. On the other hand, strong Zn (0 0 1), (101), and (102) diffraction peaks were observed at 19 cm sample location which, is indicated that the prepared sample was mainly composed of a great number of Zn with little oxidation. Whereas, very weak ZnO of (100), (002), and (101) peaks were observed in the sample located at 6 cm.

Moreover, wide width of ZnO diffraction peak at $2\theta=56.59^\circ$ indicates that the resulting products had very small size of crystalline and the resulting products were amorphous. It is noticeable that the (0 0 2) peak (at 34.3°) is overwhelming, revealing a preferred orientation of the nanowires grown on silicon substrates that was at 11 cm location and hence, reveals align nanowires as observed in the FESEM image. As a result, different ZnO morphologies were formed at different substrate locations.

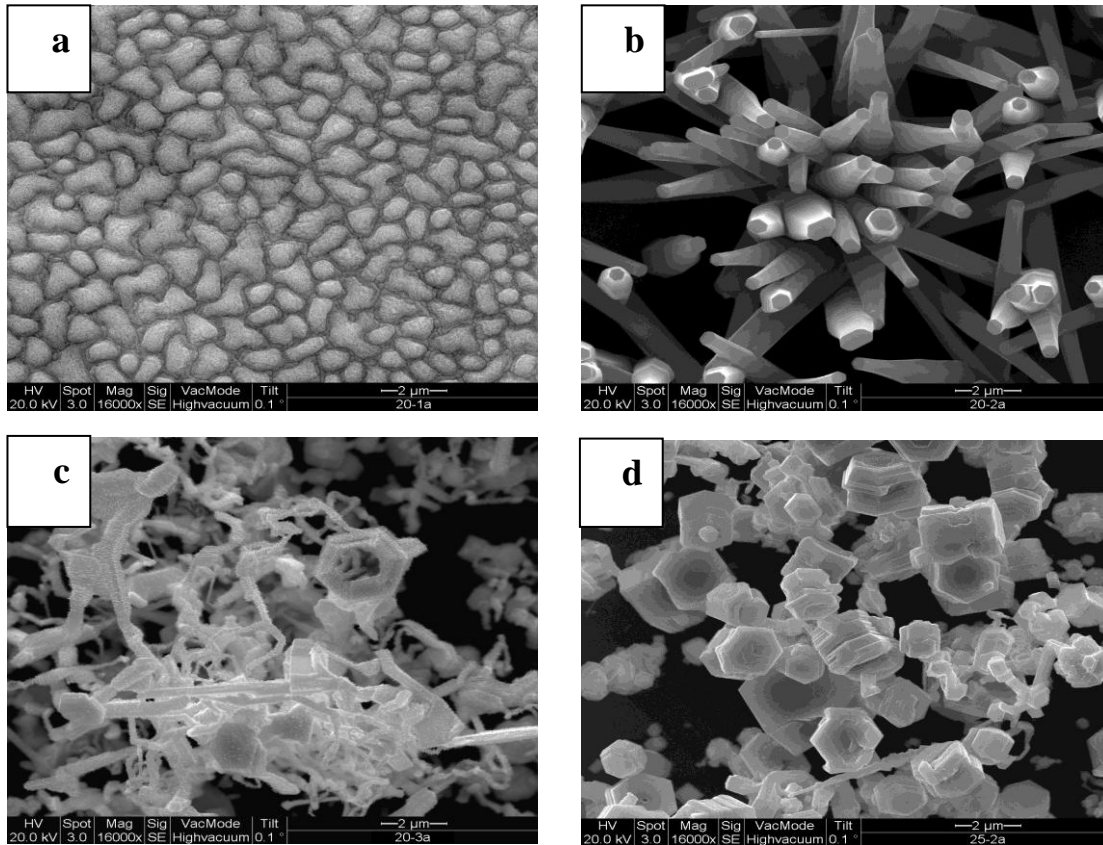


Figure 1: displays FESEM images of ZnO nanostructures grown on silicon substrates located at (a) 6cm (b) 11cm,(c) 15cm and (d)19cm from the center.

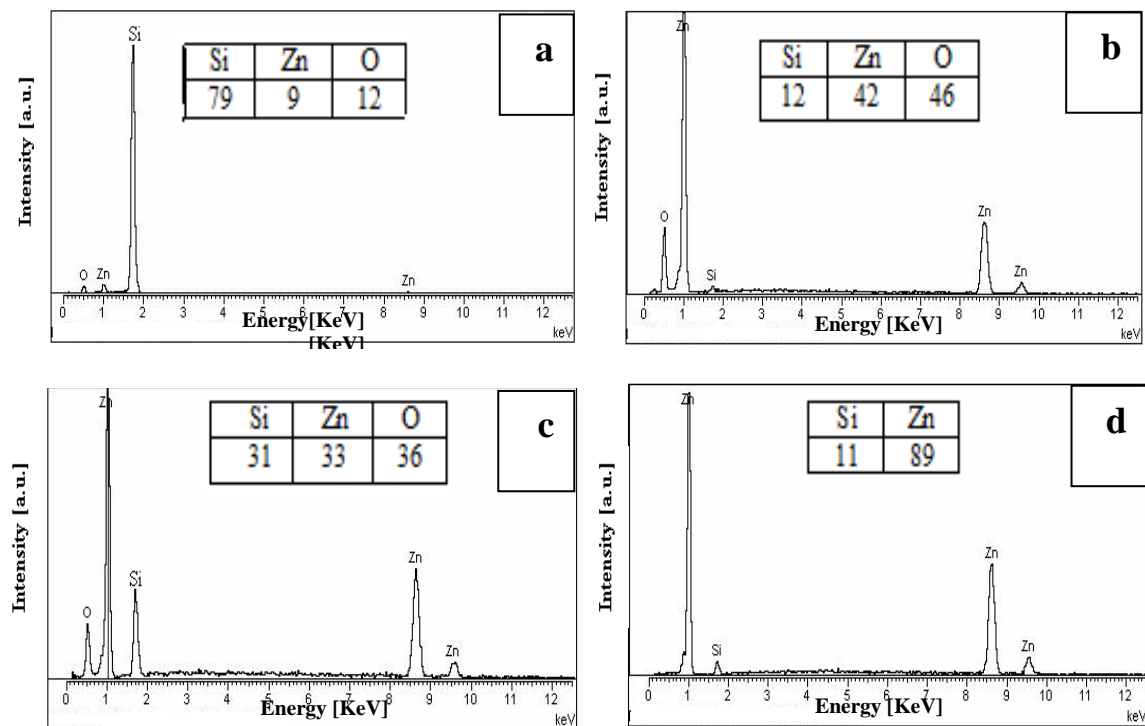


Figure 2: shows Figure 2: shows EDX spectra of ZnO nanostructures grown on silicon substrates located at (a) 6cm (b) 11cm (c) 15cm (d) 19 cm away from the center.

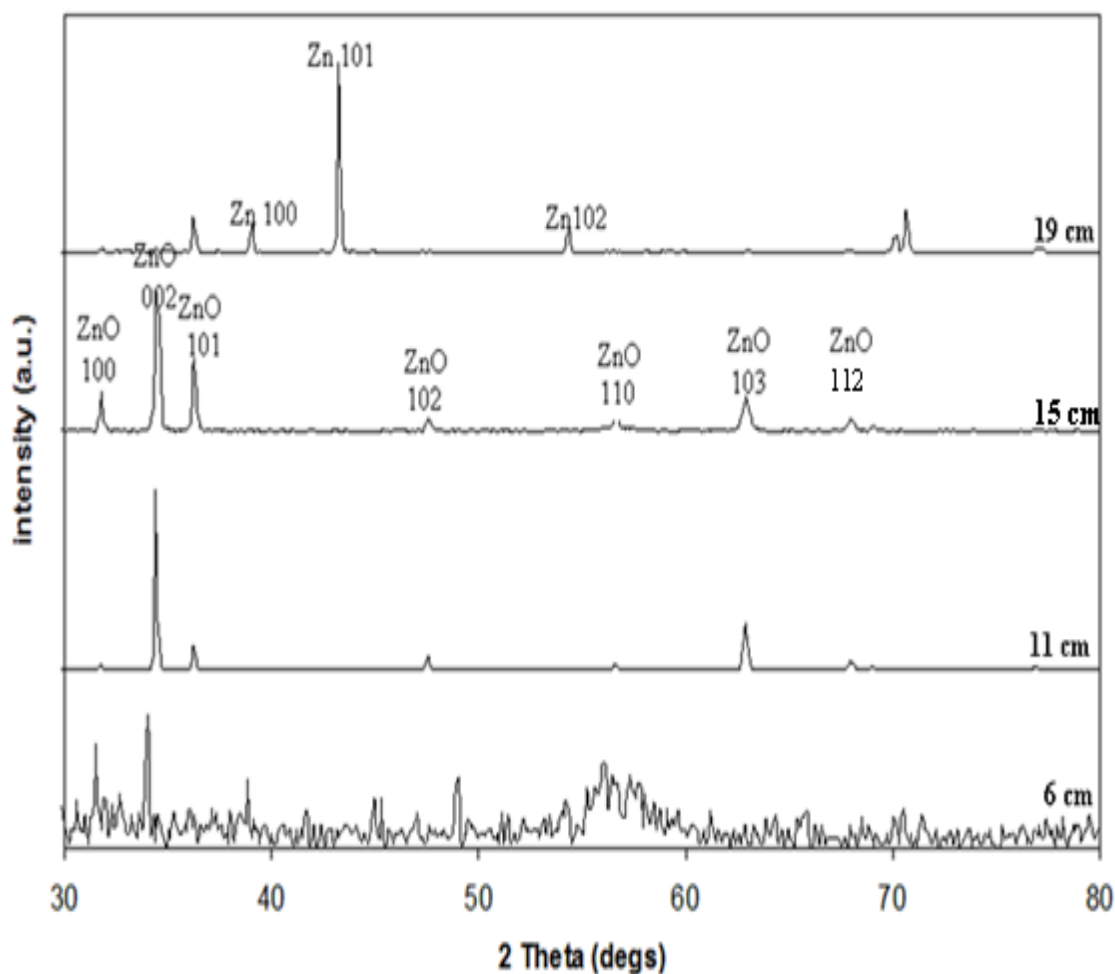


Figure 3: shows the XRD patterns of ZnO nanostructures deposited on the Si (100) substrates at different locations from the center.

Effect of deposition time

Figure 4 implies FESEM images of ZnO nanostructures grown on silicon substrates at different deposition times. Obviously, the growth density of synthesized ZnO nanostructures increases with increasing the deposition time. Figures 5 (a) and (b) display corresponding EDX spectra of 15 min and 60 min grown samples.

According to EDX results, there is no silicon peak was detected on 60 min deposition time, whereas silicon peak was observed at 15 min deposited substrate. This result gives a good evidence to the enhancement of the growth yield of ZnO nanostructures as the deposition time is increased.

When the growth time increased to 60 min, the silicon substrate was all covered with nanostructures as it shown in figure 4(d). It is

interesting to note that all the FESEM images display nanotetrapod structures.

In addition, shorter nanotetrapods with large diameters were formed as deposition time increased. In other words, shorter ZnO nanotetrapods with larger diameter are obtained at 60 min deposition time. The longest nanotetrapods legs were obtained in 15 min deposition time with 700 nm tall and 30 nm width where the largest nanotetrapods diameter which equal to 200 nm with 400 nm length was formed at 60 min deposition time.

It is worth to point out that when the deposition time increased from 45 min to 60 min, ZnO nanostructures changed from nanotetrapods to sheets form. Hence, the deposition time play a key role in control the dimensions of ZnO nanostructures.

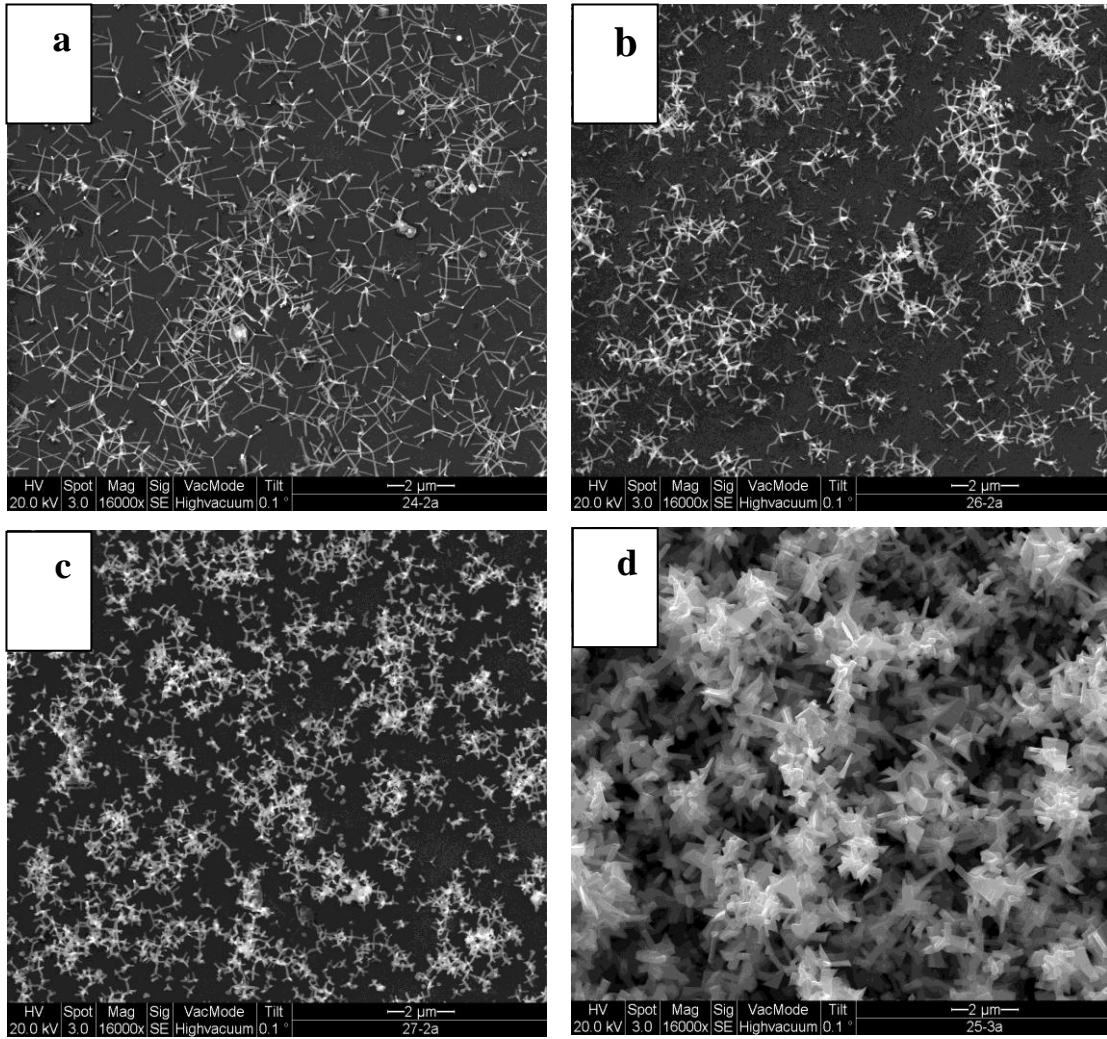


Figure 4: displays FESEM images of ZnO nanostructures formed upon silicon substrates deposited at (a) 15min (b) 30min, (c) 45min and (d) 60min deposition time.

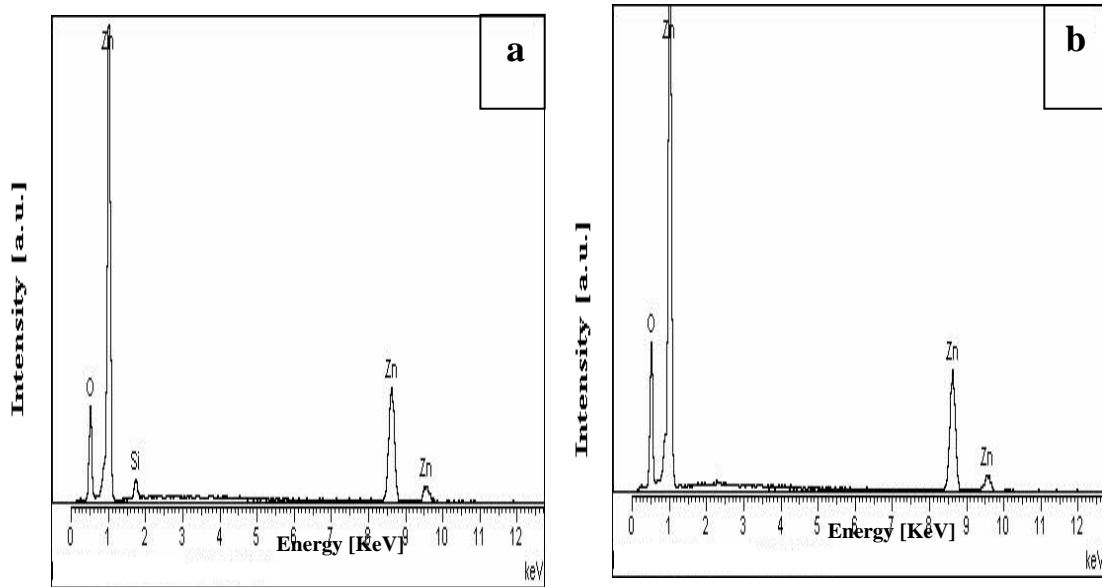


Figure 5: shows EDX spectra of ZnO nanostructures grown at (a) 15 min (b) 60 min deposition time.

Figure 6 shows typical XRD patterns of the as-synthesized ZnO nanostructures at different deposition time. No diffraction peaks of metallic Zn or other impurities can be observed besides ZnO peaks for all the grown samples. Obviously, XRD spectra reveal that as deposition time increased a high density of ZnO products formed. In addition, (100), (002) and (101) peaks have been observed and they have almost the same

intensities from 15 min to 45 min deposition time. In contrast, the highest intensity of (002) peak, at 60 min deposition time, shows that those nanostructures are grown along the c-axis direction that is normal to the substrates. As a result, the intensity of the ZnO (002) peak significantly enhances with increasing deposition time to 60 min.

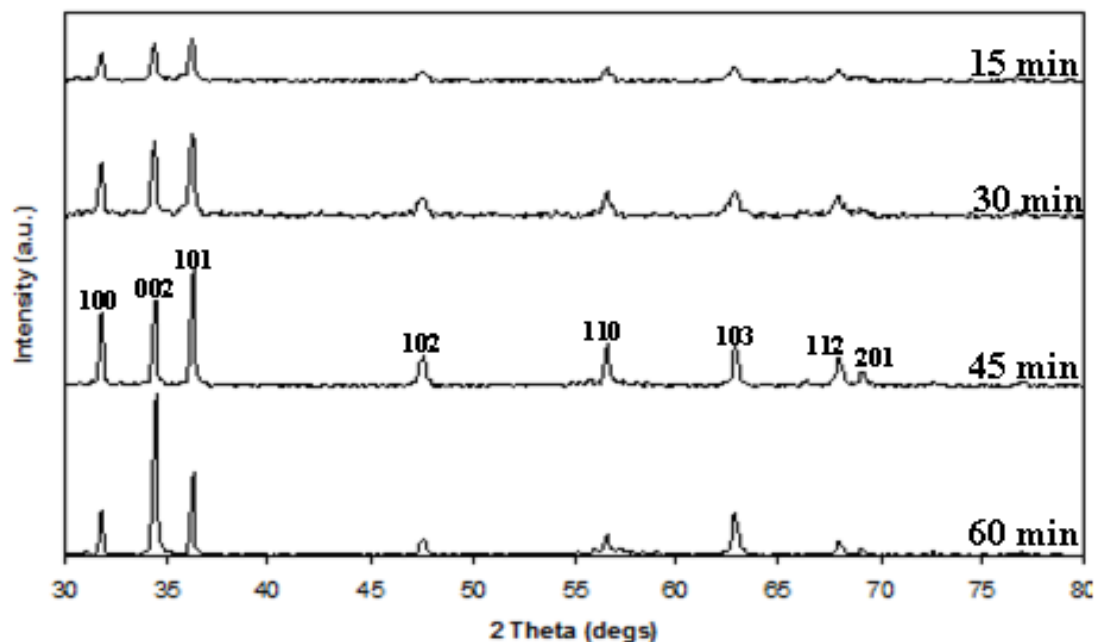
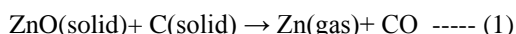


Figure 6: shows typical XRD patterns of the as-synthesized ZnO nanostructures at different deposition time.

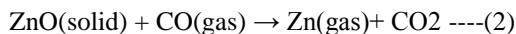
Mechanism of ZnO nanostructures growth

The growth of ZnO nanostructures without catalyst has been demonstrated by various methods. In this work, the growth mechanism can attribute to self-catalytic vapor-liquid-solid (VLS) mechanism [4], whereas Zn and Zn-suboxides functioned as self-catalysts.

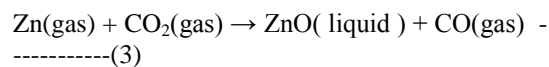
To facilitate the production of ZnO nanostructures in simple evaporation and at atmospheric pressure, the growth reduction was utilized to decompose high-melting-point 1,975°C of ZnO at lower-melting point. This happened when, ZnO powder is mixed with graphite powders to form Zn and CO gas as illustrated in Eq. (1).



Then, CO gas worked as reduction agent with ZnO powder to form more of Zn vapor and CO₂ gas as shown in Eq. (2).



Zn and CO₂ vapors were then transported or diffused to a low temperature region (downstream of carrier gas flow), which they reacted to form ZnO/ ZnO_x liquid droplets and CO gas which depart the tube as shown in Eq. (3).



Moreover, a part of the Zn vapor will condense on the substrate to form liquid droplets, which are the preferred sites to absorb ZnO or ZnO_x vapor species.

It means that the Zn/ZnO or Zn/ZnO_x liquid droplets functioned as a nucleation site for subsequent Zn and Zn-suboxides which are in vapor phase and absorb them until the droplet became supersaturated and results in ZnO segregation and nanostructures growth. On one hand, the vapor pressure of Zn, ZnO_x and CO/CO₂ was gradually decreased from the powder source location to the open side of the quartz tube. For that reason, we observed that growth yield was very low.

In addition, we believed that the Si substrate at 19 cm away from the source had low local temperature and any Zn vapor arrived to the substrate, it will solidified immediately and hence, Zn has only been obtained on Si (100).

In contrast, at the high temperature Si substrate at 6 cm away from the source, the Zn/ZnOx vapor has enough energy to keep its vapor phase and only a few particles can deposit on the edge of the growing ZnO grains resulting in ZnO film. On the other hand, as deposition time increased more vapors carried by the flow gas towards the substrate surface and hence, more dense ZnO nanostructures formed upon the substrate surface.

CONCLUSION

The dependence of ZnO nanostructures on the substrate position to the ZnO/C source confirmed the reduction-evaporation model of ZnO formation using carbothermal technique. There seem to be a define window of distances for ZnO nanostructures to be formed. For our system, the best distance was at 11 cm.

The closest distance studied yielded ZnO film and the furthest distance yielded only Zn. It was discovered that, density of ZnO increased with increasing the deposition time, which may be due the increase in the supply of Zn, ZnOx and CO/CO₂ vapors delivered to substrate by the carrier gas.

In addition, by controlling such parameters aligned ZnO nanowires with different diameters and lengths can be grown reproducibly as we have obtained them at 11cm substrate location. The average diameter of these nanowires is about 50 nm to 200 nm and the length is 4-8 μ m.

ACKNOWLEDGEMENTS

We would like to thank University Malaya (UM) for the financial support for this project (grant NO. PS303-2008C).

REFERENCES

1. Y.J. Xing, Z.H. Xi, Z.Q. Xue and X.D. Zhang. (2003). Optical properties of the ZnO nanotubes synthesized via vapor phase growth. *Appl. Phys. Lett.* 83: 1689-1691.
2. M. C. Newton, S.Firth and P.A.Warburton. (2006). ZnO tetrapod Schottky photodiodes. *Appl. Phys. Lett.* 89: 072104-072106.
3. J. Goldberger, D.J. Sirbully, M. Law and P.D. Yang. (2005). ZnO nanowire transistors. *J. Phys. Chem. B* 109: 9-14.

4. J. M. Bao, M. A. Zimmler, F. Capasso, X. W. Wang and Z. F. Ren. (2006). Broadband ZnO single-nanowire light-emitting diode. *Nano Lett.* 6:1719-1722.
5. H.Y. Dang, J. Wang and S.S. Fan. (2003). The synthesis of metal oxide nanowires by directly heating metal samples in appropriate oxygen atmospheres. *Nanotechnology* 14: 738-741.
6. Y.W. Heo, V. Varadarajan, M. Kaufman, K. Kim, D.P. Norton, F. Ren and P.H. Fleming. (2002). Site-specific growth of ZnO nanorods using catalysis-driven molecular-beam epitaxy. *Appl. Phys. Lett.* 81: 3046-3048.
7. J.-J. Wu, S.-C. Liu, C.-T. Wu, K.-h. Chen and L.-C. Chen. (2002). Heterostructures of ZnO–Zn coaxial nanocables and ZnO nanotubes. *Appl. Phys. Lett.* 81: 1312-1314.
8. B.D. Yao, Y.F. Chan and N. Wang. (2002). Formation of ZnO nanostructures by a simple way of thermal evaporation. *Appl. Phys. Lett.* 81: 757-759.
9. Y.B. Li, Y. Bando, T. Sato and K. Kurashima. (2002). ZnO nanobelts grown on Si substrate. *Appl. Phys. Lett.* 81: 144-146.
10. L. L. Zhang, C.X. Guo, J.G. Chen and J.T. Hu. (2005). The synthesis of one-dimensional controllable ZnO microrods. *Chin. Phys.* 14: 586-591.
11. J. Chen, X.W. Sun and C.X. Xu. (2004). Fabrication of zinc oxide nanostructures on gold-coated silicon substrate by thermal chemical reactions vapor transport deposition in air. *Ceramics International* 30: 1725-1729.
12. V. A. L. Roy, A. B. Djuriši , W. K. Chan, J. Gao, H. F. Lui and C. Surya. (2003). Luminescent and structural properties of ZnO nanorods prepared under different conditions. *Appl. Phys. Lett.* 83:141-143.
13. A.B. Djurišić, Y.H. Leung, W.C.H. Choy, K.W. Cheah and W.K. Chan. (2004). Visible photoluminescence in ZnO nano-tetrapod and multipod structures. *Appl. Phys. Lett.* 84: 2635-2637.
14. Z.R. Dai, Z.W. Pan and Z.L. Wang. (2003). Novel nanostructures of functional oxides synthesized by thermal evaporation. *Adv. Funct. Mater.* 13: 9-24.
15. W. D. Yu, X. M. Li and X. D. Gao. (2004). Self-catalytic synthesis and photoluminescence

- of ZnO nanostructures on ZnO nanocrystal substrates. *Appl. Phys. Lett.* 84: 2658-2660.
16. Z. W. Pan, Z. R. Dai and Z. L. Wang. (2001). Nanobelts of semiconducting oxides. *Science* 291: 1947-1949.
17. Y. Dai, Y. Zhang, Q. K. Li and C. W. Nan (2002). Synthesis and optical properties of tetrapod-like zinc oxide nanorods. *Nan. Chem. Phys. Lett.* 358: 83-86.
18. JCPDS-International center for diffraction data, Card No. 03-0888.